Maintenance Mechanism of a 24 May 2000 Supercell Storm Developing in Moist Environment over the Kanto Plain, Japan

*Shingo Shimizu[1], Hiroshi Uyeda[1], Qoosaku Moteki[1], Takeshi Maesaka[2], Yoshimasa Takaya[3], Kenji Akaeda[3], Teruyuki Kato[3], Masanori Yoshizaki[3]
[1] Hydrospheric Atmospheric Research Center, Nagoya University, [2] Graduate School of Science, Hokkaido University, [3] Meteorological Research Institute, JMA

1. Introduction

A supercell storm developing in a moist environment was investigated in order to understand its development and maintenance mechanism. A supercell storm in a moist environment was observed by two C-band Doppler radars on 24 May 2000 over the Kanto Plain, Japan. This storm was investigated by using dual Doppler analyses and numerical simulations with the MRI-NHM (Meteorological Research Institute Non-Hydrostatic Model (Saito et al., 2001)). The purpose of this paper is to reveal the development and maintenance mechanism of a supercell storm developing in a moist environment compared with that in a dry environment as in the Great Plains.

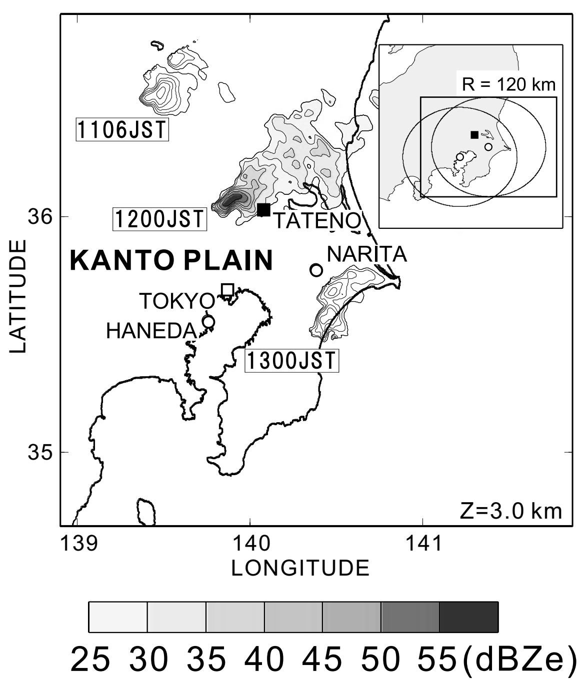

Fig. 1. The locations of two Doppler radars (Narita and Haneda airports), and the radar reflectivity fields at a height of 3 km from 1106 JST to 1300 JST on 24 May 2000. The gray scale shows reflectivity at 1200 JST. The contour (over 30 dBZe every 5 dBZe) shows reflectivity at 1106 JST and 1300 JST. The observation area of the Doppler radars (120 km in radius) is shown in a box at the upper-right corner.

* Corresponding author address: Shingo Shimizu, Hydrospheric Atmospheric Research Center, Nagoya University, Nagoya 464-8601, Japan
Email: s010125m@mbox.media.nagoya-u.ac.jp

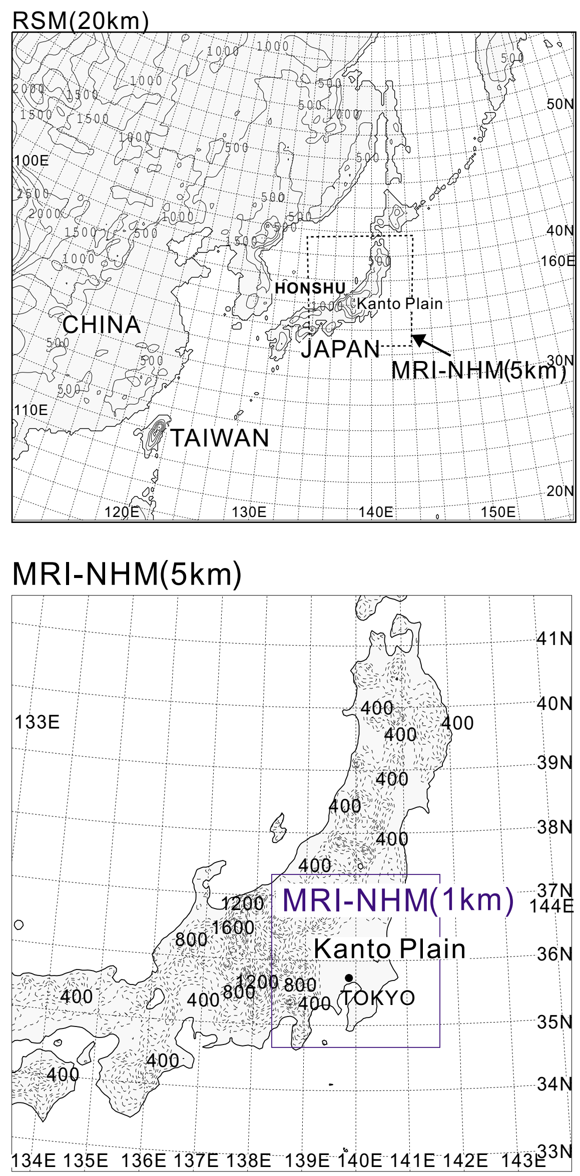

Fig. 2. The domains for the numerical simulations. The 5km-NHM (dashed square in Fig. 2a) was one-way nested within the output of the Regional Spectrum Model (on the top). The 1km-NHM (solid square in Fig. 2b) was one-way nested within the outputs of the 5km-NHM (on the bottom).

2. Data and model description

The locations of the radar sites (Narita and Haneda airports) and the upper-air sounding at Tateno are shown in Fig. 1. Two C-band Doppler radars, covering a 120 km in radius over the Kanto Plain (Fig. 1,upper right), recorded sets of volume scan data regarding reflectivity and Doppler velocity every six or seven minutes. Upper-air soundings of wind, temperature, and humidity at 900 JST were obtained from the Tateno Aerological Observatory of Japan Meteorological Agency (JMA). Surface temperature, wind speed and direction, and precipitation amounts were available every 10 minutes from surface stations of the AMeDAS (Automated Meteorological Data Acquisition System of JMA) at Koga and Sakura.

The numerical simulations were conducted with a 1km-resolution MRI-NHM (1km-NHM). The 1km-NHM was one-way nested within the outputs of a 5km-NHM (Fig .2). The 5km-NHM was also one-way nested within the outputs of a 20 km resolution Regional Spectrum Model.

3. Results of dual Doppler analyses

A storm which developed in a pressure trough was observed by two Doppler radars from 1106 JST to 1400 JST on 24 May 2000 over the Kanto Plain. The radar reflectivity fields from 1106 JST to 1300 JST, derived from Narita airport radar, are shown in Fig. 1.

A remarkable hook echo, which is the main feature of a typical supercell storm developing over the Great Plains (e.g., Browning and Foote, 1976), was observed southwest of the storm from 1144 JST to 1212 JST (Fig. 3). A square in Fig. 3 indicates an analysis area ($20km \times 20km$) for a vertical profile in Fig. 4. This analysis area chased the center of the updraft core at a height of 3 km above sea level (ASL) from 1106 JST to 1400 JST in order to investigate the time series of the maximum reflectivity profile in the analysis area.

The time series of the maximum reflectivity profile in the traced square from 1106 JST to 1400 JST is shown in Fig. 4. A strong echo over 60 dBZe was observed at about 5 km ASL just before 1200 JST. This echo descended to the ground from 1200 JST to 1300 JST. This remarkable development in reflectivity at 1200 JST was accompanied by a strong updraft (over 8 $m\ s^{-1}$) and strong vertical vorticity (over $1.0 \times 10^{-2} s^{-1}$) at a height of 5 km ASL (not shown).

Radar reflectivity at 1200 JST overlaid with storm-relative wind vectors and updraft velocity (by contour) at a height of 3 km ASL is shown in Fig. 5. There was an updraft core (over 8 m s^{-1}) in the center of the hook echo. The dashed arrow near the hook indicates cyclonic flow with strong vertical vorticity over $3.0 \times 10^{-3} s^{-1}$. The vorticity center colocated with the updraft core at an altitude of 3 km to 5 km ASL.

A vertical cross section along the A-A' line (Fig.

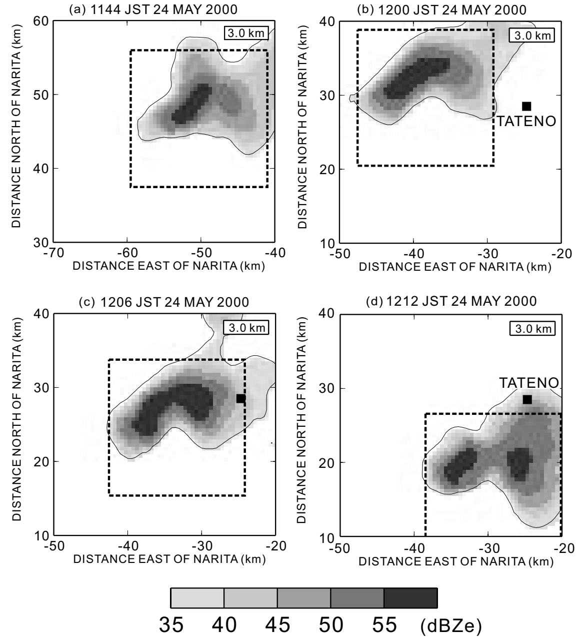

Fig. 3. Hook-shaped reflectivity at a height of 3 km ASL from 1144 JST to 1212 JST. A square (20×20 km) indicates an analysis area for a vertical profile in Fig. 4.

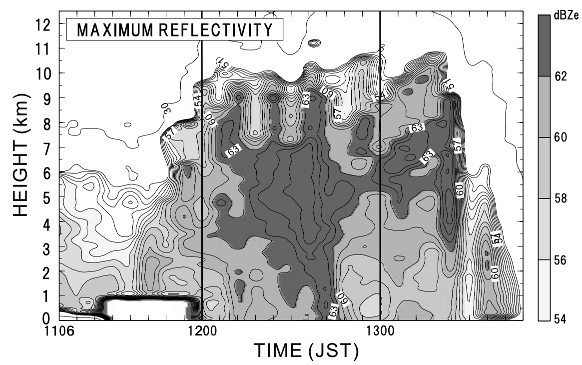

Fig. 4. The time-height cross-section of the maximum reflectivity in the analysis area in Fig. 3 from 1106 JST to 1400 JST.

5) through the center of the updraft core is shown in Fig. 6. A strong echo, over 45 dBZe, was overhanging ahead of the storm. In Fig. 6, the open arrow shows the location of a strong updraft core. Inflow from the southeast turned into an updraft at the location of the open arrow.

These results of dual Doppler analyses reveal that this supercell storm had characteristics similar to those of a typical supercell storm: an overhanging structure and an updraft core colocating with the vorticity center.

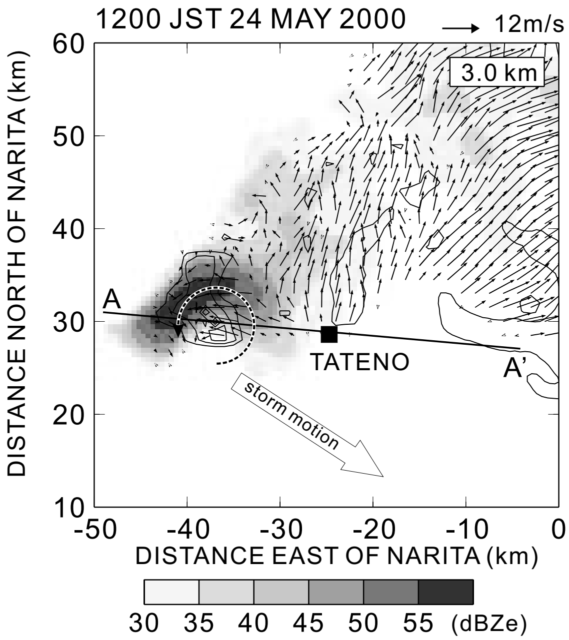

Fig. 5. Radar reflectivity over 30 dBZe overlaid with storm-relative wind vectors and updraft velocity (solid contour every 2 $m\ s^{-1}$, starting from 2 $m\ s^{-1}$) at a height of 3 km ASL. There was a strong updraft core in the center of a remarkable hook echo. The dashed arrow near the hook echo indicates cyclonic flow with strong vertical vorticity over $3.0 \times 10^{-3} s^{-1}$. The open arrow indicates storm motion south-eastward with 50 $km\ h^{-1}$. A vertical cross section along the A-A' line is shown in Fig. 6.

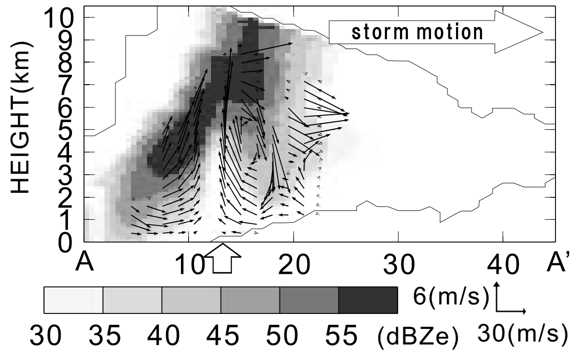

Fig. 6. A vertical cross section along the A-A' line in Fig. 5. A strong echo over 45 dBZe was overhanging ahead of the storm. The open arrow indicates the location of an updraft core.

4. Results of 1km-NHM

We conducted numerical simulations with the 1km-NHM in order to clarify precipitation particle in the strong overhanging echo region (over 45 dBZe) and to investigate the flow structure around the storm where Doppler radar could not detect an echo. Features of the storm observed by Doppler radar were reproduced well by the 1km-NHM, as shown in Fig. 7. However, the simulated storm shifted 30 km north and developed one hour later than the observed storm. The mixing ratio of rain (Qr) overlaid with storm-relative wind at a height of 3 km ASL at 1200 JST is shown in Fig. 7. The distribution of Qr over 2 $g\ kg^{-1}$ was similar to the shape of the hook echo observed by radar, as shown in Fig. 5. The dashed arrow indicates cyclonic flow with strong vorticity existing at the southwest of the hook, as shown in Fig. 5.

A vertical cross section of Qr and Qg along the line A-A' through the center of vorticity is shown in Fig. 8. The contour indicates a mixing ratio of graupel (Qg), the gray scale indicates Qr. The open arrow shows the location of the updraft core. Corresponding to the overhanging echo structure observed by radar, two cores of Qg over 8 $g\ kg^{-1}$ are shown at both the front and rear of the updraft core. The particles in the two cores of Qg seem to be hail because the two Qg cores correspond to the strong echo (over 55 dBZe).

With regard to flow structure, inflow from the southeast of the storm existed less than approximately 2 km ASL ahead of the storm. As depicted in Fig. 8, the inflow turned into an updraft at the location of the open arrow. Behind the storm, the westerly wind turned to a downdraft below 8 km ASL, as shown in Fig. 9. Corresponding to the rear Qg core in Fig. 8, a downdraft core over -4 $m\ s^{-1}$ induced by loading existed at a height of 6 km ASL in Fig. 9. Another downdraft core over -2 $m\ s^{-1}$ induced by evaporation cooling existed below 3 km ASL in Fig. 9. This downdraft below 3 km ASL produced a surface outflow in the rainshaft corresponding to Qr over 1 $g\ kg^{-1}$, as shown in Fig. 8. Vertical shear between the surface and an altitude of 3 km ASL (0°C level) was strong over $6.8 \times 10^{-3}\ s^{-1}$ as represented by the solid circle in Fig. 7.

These characteristics of the storm are very similar to those of a typical supercell storm. However, a considerable difference between this storm and the typical supercell storm is that the downdraft below 3 km ASL was relatively weak (less than 3 $m\ s^{-1}$). The cause of the weak downdraft is discussed in the next section.

5. Discussion

In a previous study (Klemp, 1987), it was found that two factors act to extend the longevity of a supercell storm in a dry and strong shear environment. First, a strong storm-relative low-level inflow prevents the gust front from moving out of the storm (Wilhelmson and Klemp, 1978b; Thorpe and Miller, 1978; Weisman and Klemp, 1982). Second, lifting pressure gradients induce an updraft growth almost directly above the surface gust front (Schlesinger, 1980; Rotunno and Klemp, 1982).

A first necessary condition for the development of a steady storm such as a supercell storm is that

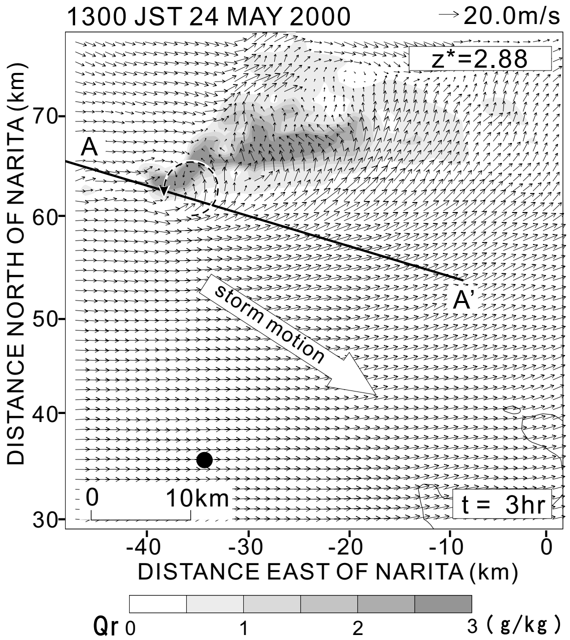

Fig. 7. The simulated supercell storm at 1200 JST 24 May 2000. The mixing ratio of rain (gray scale) overlaid with storm-relative wind vectors. The dashed arrow indicates strong vertical vorticity, as shown in Fig. 5. A vertical cross section along the A-A' line is shown in Fig. 8 and Fig. 9. Vertical shear between the surface and an altitude of 3 km ASL was over $6.8 \times 10^{-3} s^{-1}$ as represented by the solid circle in Fig. 7.

the storm-relative inflow be strong enough to keep the outflow from propagating away from the updraft. If the inflow is weak, the gust front may move ahead of the storm, and the supply of warm air to the updraft may be cut off (Weisman and Klemp, 1982). This theory, developed during previous studies is consistently supported in a dry environment. Because the downdraft in a dry environment is often very strong due to evaporation cooling, the strength of inflow is the most important factor in a steady storm. However, in a moist environment, the downdraft is not always strong. Therefore, the balance of the inflow and outflow strength is the most important factor.

In the present case, the upper-air sounding at Tateno a few hours before the development of the storm under discussion is shown in Fig. 10. A dry layer existed from 650 hPa to 500 hPa. A melting layer existed at 680 hPa (about 3 km ASL). Below the melting layer, there was a relatively moist layer (relative humidity over 70%). Because of this moist layer, the production of negative buoyancy by evaporation cooling was limited. This explains why the temperature had fallen only 3 degrees when the core of the storm passed over the AMeDAS surface station at Koga (Fig. 11). Because negative buoyancy by evaporation cool-

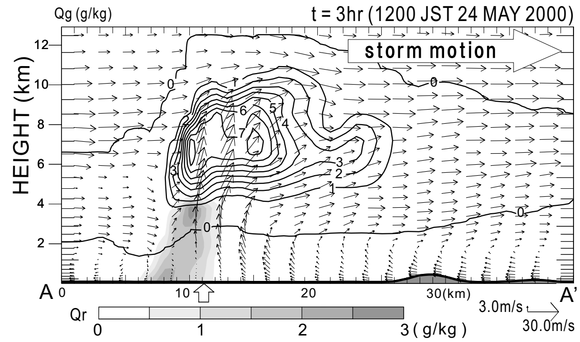

Fig. 8. A vertical cross section along the A-A' line in Fig. 7 of Qg and Qr. The gray scale indicates Qr, and the contour (every 1 $g\ kg^{-1}$) indicates Qg. The open arrow indicates the location of an updraft core.

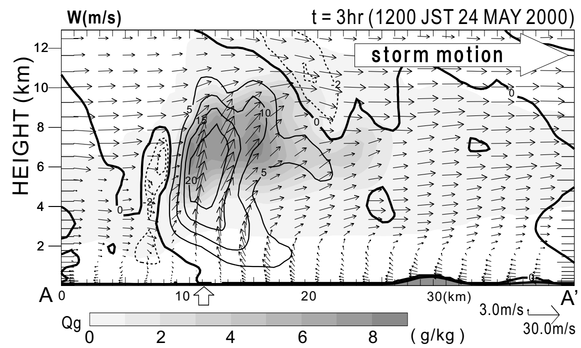

Fig. 9. A vertical cross section along the A-A' line in Fig. 7 of Qg and vertical wind velocity. The gray scale indicates Qg, and the contour indicates vertical wind velocity. The contour interval of an updraft is 5 $m\ s^{-1}$ (solid contours), and the dashed contours represent a downdraft every -2 $m\ s^{-1}$.

ing was small, the downdraft below the melting layer was relatively weak. The surface outflow produced by the weak downdraft balanced the storm-relative inflow at the location indicated by the open arrow in Fig. 9.

Regarding a second necessary condition for the development, Weisman and Klemp (1982) revealed that mid-level vertical vorticity develops in a strong shear environment. Rotunno and Klemp (1982) found that mid-level vertical vorticity is derived from the horizontal vorticity of the environmental shear and that the vertical vorticity induces lifting pressure gradients, which lower the pressure and thereby induce updraft growth.

In the present case, the vertical shear was strong ($6.8 \times 10^{-3}\ s^{-1}$) and the vertical vorticity was over $1.0 \times 10^{-2} s^{-1}$ at a height of 5 km ASL. Therefore, the lifting pressure gradients maintained a strong updraft.

Before 1230 JST, the weak outflow balanced the storm-relative inflow with the horizontal vorticity of the environmental shear above the surface

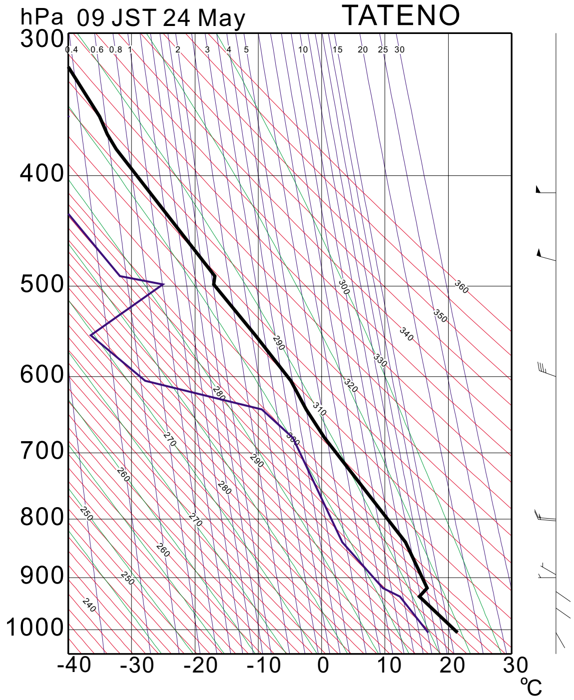

Fig. 10. The upper-air sounding at Tateno at 900 JST. Profiles of temperature (thick solid line), dew-point temperature (thin solid line), and wind speed and direction (on the right).

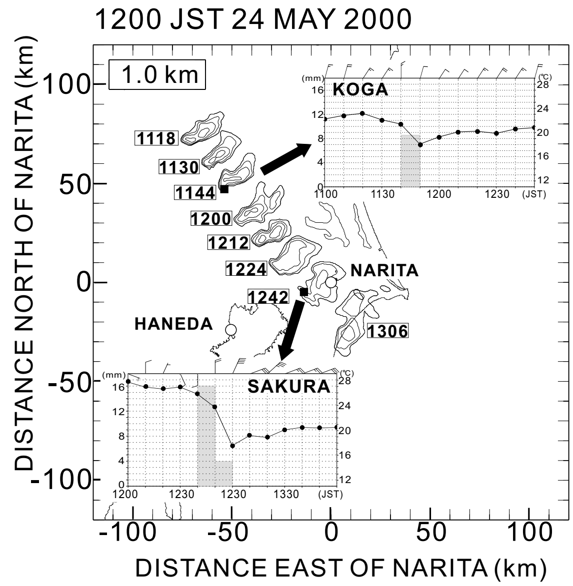

Fig. 11. Reflectivity over 45 dBZe at a height of 1 km ASL from 1118 JST to 1306 JST and traces of surface temperature (solid line), wind speed and direction, and precipitation amounts at Sakura and Koga (solid square).

gust front. The inflow turned into an updraft with strong vertical vorticity of over $1.0 \times 10^{-2} s^{-1}$. This strong vertical vorticity induced lifting pressure gradients and maintained the updraft. Therefore before 1230 JST, the storm had characteristics similar to those of a typical supercell storm (except for weak downdraft).

After 1230 JST, the storm could not maintain a steady updraft. Negative buoyancy above the melting layer gradually got stronger as the mass of hail and graupel increased. The downdraft above the melting layer brought dry air between 650 hPa and 500 hPa to the relatively moist layer below 3 km ASL. As the layer below 3 km ASL was drier, evaporation cooling worked more effectively. The temperature had fallen 9 degrees when the core of the storm passed over the AMeDAS station at Sakura, as shown in Fig. 11. Therefore, the outflow was stronger because the environment was drier below the melting layer, and the gust front spread (not shown), and the steady updraft could not be maintained. At 1306 JST, a new cell appeared to the south of the storm, as shown in Fig. 11.

In a previous numerical study (Weisman and Klemp, 1982), convective available potential energy (CAPE) and vertical shear as environmental conditions controlled the strength of the downdraft. Greater instability, as measured by CAPE, was found to increase storm downdraft strength. This is because a stronger updraft can suspend larger rain amounts that create greater evaporation cooling and precipitation loading, resulting in a stronger downdraft (Weisman and Klemp, 1982; Weisman and Klemp, 1984). In addition, weaker unidirectional wind shear was found to produce stronger downdraft (Wilhelmson and Klemp, 1978a). However, studies that have investigated the affect of mid-tropospheric dryness were very few (Gilmore and Wicker, 1998). The efficiency of evaporation cooling is controlled by the dryness below the melting layer.

In the present case, when the layer below the melting layer was moist, before 1230 JST, evaporation cooling did not work effectively, and the outflow was so weak that it could balance the storm-relative inflow. When the layer below the melting layer was drier, after 1230 JST, evaporation cooling worked effectively and the outflow was so strengthened that it propagated away from the updraft. Thus, the strength of the outflow is controlled by efficiency of evaporation cooling. Therefore, in investigating the balance of the inflow and outflow strength, the profile of relative humidity is an important environmental factor to consider.

6. Conclusions

A conceptual model of the 24 May 2000 supercell storm observed over the Kanto Plain is shown in Fig. 9a. The structure of this storm (Fig. 9a) was similar to that of a typical supercell storm (Fig. 9b), with an overhang structure, an updraft core with vertical vorticity near the altitude of the melting layer, and strong vertical shear in the lower layer. However, the downdraft behind the storm and the outflow were very weak in the supercell storm of 24 May 2000 because of the moist environment below the melting layer before 1230 JST. This weak outflow balanced the storm-relative inflow with the horizontal vorticity of the environmental vertical shear. The inflow turned into an updraft with mid-level vertical vorticity. Lifting pressure gradients induced by strong mid-level vertical vorticity maintained the updraft core ahead of the gust front.

A supercell storm on 24 May 2000 had similarities to that in a dry environment over the Great Plains. Even in a moist environment, the balance of the outflow and the inflow was an important factor for the development and maintenance of the supercell storm. Additional research is needed to investigate the strength of outflow and the influence of the mid-level humidity in a moist environment.

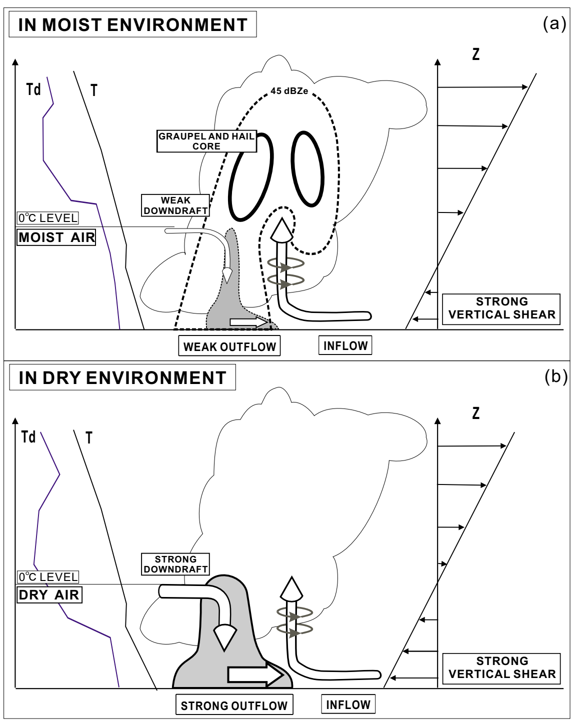

Fig. 12. Conceptual models of (a) the 24 May 2000 supercell storm developing in a moist environment and (b) a typical supercell storm developing in a dry environment over the Great Plains.

Acknowledgments. The authors would like to express their special thanks to Haneda and Narita airports for providing radar data. The numerical simulations were performed on the Hitachi SR-8000 at the Hokkaido University Computing Center.

REFERENCES

Browning, K. A. and G. B. Foote, 1976: Airflow and hail growth in supercell storms and some implications for hail suppression. *Quart. J. R. Soc.*, **102**, 499–533.

Gilmore, M. S. and L. J. Wicker, 1998: The influence of midtropospheric dryness on supercell morphology and evolution. *Mon. Wea. Rev.*, **126**, 943–958.

Klemp, J. B., 1987: Dynamic of tornadic thunderstorms. *Annu. Rev. Fluid. Mech.*, **19**, 369–402.

Rotunno, R. and J. B. Klemp, 1982: The influence of the shear-induced pressure gradient on thunderstorm motion. *Mon. Wea. Rev.*, **110**, 136–151.

Saito, K., T. Kato, H. Eito and C. Muroi, 2001: Documentation of meteorological research institute numerical prediction division unified nonhydrostatic model. Technical report, Meterological reserch institute,Japan.

Schlesinger, R. E., 1980: A three-dimensional numerical model of an isolated deep thunderstorm .Part II: Dynamics of updraft splitting and mesovortex couplet evolution. *J. Atoms. Sci.*, **37**, 395–420.

Thorpe, A. J. and M. J. Miller, 1978: Numerical simulations showing the role of the downdraught in cumulonimbus motion and splitting. *Quart. J. R. Met. Soc.*, **104**, 873–893.

Weisman, M. L. and J. B. Klemp, 1982: The dependence of numerically simulated convective storms on vertical wind shear and buoyancy. *Mon. Wea. Rev.*, **110**, 504–520.

Weisman, M. L. and J. B. Klemp, 1984: The structure and classification of numerically simulated convective storms in directionally varying wind shears. *Mon. Wea. Rev.*, **112**, 2479–2499.

Wilhelmson, R. B. and J. B. Klemp, 1978a: A numerical study of storm splitting that leads to long-lived storms. *J. Atmos. Sci.*, **35**, 1974–1986.

Wilhelmson, R. B. and J. B. Klemp, 1978b: A three-dimensional numerical simulation of splitting that leads to long-lived storms. *J. Atmos. Sci.*, **35**, 1037–1063.